

Two Endoplasmic Reticulum (ER)/ER Golgi Intermediate Compartment-based Lysine Acetyltransferases Post-translationally Regulate BACE1 Levels^{*[5]}

Received for publication, June 26, 2008, and in revised form, November 13, 2008 Published, JBC Papers in Press, November 14, 2008, DOI 10.1074/jbc.M804901200

Mi Hee Ko[‡] and Luigi Puglielli^{‡§1}

From the [‡]Department of Medicine, University of Wisconsin-Madison and [§]Geriatric Research Education Clinical Center, Veterans Affairs Medical Center, Madison, Wisconsin 53705

We have recently identified a novel form of post-translational regulation of BACE1 (β -site amyloid precursor protein-cleaving enzyme 1), a membrane protein that acts as the rate-limiting enzyme in the generation of the Alzheimer disease amyloid β -peptide. Specifically, nascent BACE1 is transiently acetylated in seven lysine residues clustered in a highly disordered region of the protein that faces the lumen of the endoplasmic reticulum (ER)/ER Golgi intermediate compartment (ER/ERGIC). The acetylation protects the nascent protein from degradation by PCSK9/NARC-1 in the ERGIC and allows it to reach the Golgi apparatus. Here we report the identification of two ER/ERGIC-based acetyltransferases, ATase1 and ATase2. Both proteins display acetyl-CoA:lysine acetyltransferase activity, can interact with and acetylate BACE1, and display an ER/ERGIC localization with the catalytic site facing the lumen of the organelle. Both ATase1 and ATase2 regulate the steady-state levels of BACE1 and the rate of amyloid β -peptide generation. Finally, their transcripts are up-regulated by ceramide treatment. In conclusion, our studies have identified two new enzymes that may be involved in the pathogenesis of late-onset Alzheimer disease. The biochemical characterization of the above events could lead to the identification of novel pharmacological strategies for the prevention of this form of dementia.

The efficiency of folding, conformational maturation, and molecular stability of nascent membrane and secretory proteins is greatly affected in the endoplasmic reticulum (ER)² by

post-translational events that modify, either temporally or definitively, the protein (1). One of the best characterized forms of transient modification is the attachment of a glucose residue to improperly folded nascent glycoproteins by the UDP-glucose:glycoprotein glucosyltransferase (2, 3). This transient event regulates the interaction of the nascent protein with the chaperone calnexin and its ability to leave the early secretory pathway. The mechanism works in such a way that successfully folded proteins dissociate from the calnexin/calreticulin cycle and advance toward the Golgi apparatus, whereas misfolded intermediates are directed toward the ER-associated degradation system (1, 4).

We have recently reported the identification of a novel form of post-translational regulation of BACE1 (β -site APP-cleaving enzyme 1) (5), a membrane protein that acts as the rate-limiting enzyme in the generation of the Alzheimer disease amyloid β -peptide ($A\beta$) from the amyloid precursor protein (APP). Specifically, nascent BACE1 is transiently acetylated in seven lysine residues clustered in a highly disordered region of the protein that faces the lumen of the ER and ER Golgi intermediate compartment (ERGIC). The lysine acetylation of nascent BACE1 regulates its ability to advance toward the Golgi apparatus, where a Golgi-based deacetylase removes the acetyl groups. Nonacetylated intermediates of the nascent protein are retained in the early secretory pathway and degraded by a mechanism that involves the serine protease PCSK9/NARC-1 (proprotein convertase subtilisin kexin-type 9/neural apoptosis-regulated convertase-1) (6). The acetylation of nascent BACE1 in the lumen of the ER and/or ERGIC requires a membrane transporter that translocates acetyl-CoA, the donor of the acetyl group, from the cytoplasm to the lumen of the ER, and one or more ER/ERGIC-based acetyl-CoA:lysine acetyltransferases (5).

The acetylation/deacetylation process is tightly regulated by the lipid second messenger ceramide (5, 7, 8) and is under the control of the general aging program mediated by the insulin-like growth factor 1 receptor (IGF-1R) (9, 10). Ceramide, the last output of the above pathway, regulates both efficiency of acetylation in the lumen of the ER/ERGIC and rate of deacetylation in the Golgi apparatus (5). As a result, the hyperactivation of ceramide signaling that occurs during normal aging (8) or in progeroid-like animal models (9) leads to increased acetylation and steady-state levels of BACE1 and to increased production of $A\beta$ (8, 9). The relevance of the above events for AD neuropathology is stressed by the fact that aging is the single most

* This work was supported, in whole or in part, by a National Institutes of Health grant (to L.P.). The costs of publication of this article were defrayed in part by the payment of page charges. This article must therefore be hereby marked "advertisement" in accordance with 18 U.S.C. Section 1734 solely to indicate this fact.

[5] The on-line version of this article (available at <http://www.jbc.org>) contains supplemental Methods, Figs. 1–3, and additional references.

The nucleotide sequence(s) reported in this paper has been submitted to the GenBank™/EBI Data Bank with accession number(s) NM_016347 and NM_003960.

¹ To whom correspondence should be addressed: Dept. of Medicine, University of Wisconsin-Madison, VAH-GRECC 11G, 2500 Overlook Terrace, Madison, WI 53705. Tel.: 608-256-1901 (Ext. 11569); Fax: 608-280-7291; E-mail: lp1@medicine.wisc.edu.

² The abbreviations used are: ER, endoplasmic reticulum; ERGIC, ER Golgi intermediate compartment; APP, amyloid precursor protein; BACE1, β -site APP-cleaving enzyme 1; AD, Alzheimer disease; $A\beta$, amyloid β -peptide; siRNA, short interfering RNA; GAPDH, glyceraldehyde-3-phosphate dehydrogenase; BisTris, 2-[bis(2-hydroxyethyl)amino]-2-(hydroxymethyl)propane-1,3-diol; CHO, Chinese hamster ovary; HAT, histone acetyltransferase.

important risk factor for late-onset AD and that AD patients have very high levels of ceramide in the brain, when compared with age-matched controls (reviewed in Ref. 10).

Here we report the identification of two ER/ERGIC-based acetyltransferases, which we named ATase1 and ATase2. Both proteins display acetyl-CoA:lysine acetyltransferase activity *in vitro* and under native conditions can interact with and acetylate BACE1 *in vitro* and *in vivo*, and show an ER/ERGIC localization. They both regulate the steady-state levels of BACE1 and the generation of A β , and are up-regulated by ceramide treatment of cultured cells.

EXPERIMENTAL PROCEDURES

The following experimental procedures, which have been extensively described in our previous work, are in the supplemental Methods: cell cultures and cell treatment; cell extraction, immunoprecipitation, and affinity purification; subcellular fractionation; A β determination; and siRNA treatment.

cDNA, Antibodies, and Western Blot Analysis—The cDNA for ATase1 and ATase2 was obtained from Origene (catalog number SC311351 and catalog number SC108791, respectively). Western blotting was performed on a 4–12% BisTris SDS-PAGE system (NuPAGE; Invitrogen) as described (5, 7–9, 11, 12). The following antibodies were used in this study: anti-BACE1 N-terminal (monoclonal, R & D Systems); anti-BACE1 C-terminal (polyclonal, Abcam); anti-acetylated lysine (monoclonal, Abcam; polyclonal, Cell Signaling); anti-calreticulin (ER marker; polyclonal, Abcam); anti-ERGIC-53 (ERGIC marker; polyclonal, Sigma); anti-syntaxin (Golgi marker; monoclonal, Abcam); anti-EEA1 (endosomal marker; monoclonal, BD Transduction Laboratories); anti-Myc (polyclonal, Sigma); anti-C99 (monoclonal, MBL); flotillin 2 (polyclonal; Cell Signaling); and anti-actin (polyclonal, Cell Signaling). Secondary antibodies (Amersham Biosciences) were used at a 1:6000 dilution. Binding was detected by chemiluminescence (LumiGLO kit; Kirkegaard & Perry Laboratories, Gaithersburg, MD). In some cases, the bands corresponding to BACE1 were also validated with the BACE1-Cat1 antibody (generous gift from Dr. Robert Vassar (13)).

Pixel densities (for signal area) of scanned images were calculated with Adobe Photoshop; densitometry (for signal-density) was analyzed with the EpiChemi3 DarkroomTM (UVP Bio-imaging Systems) using Labworks Image Acquisition and Analysis Software 4.5. Additionally, samples were also imaged and quantified using the Odyssey Infrared Imaging System (LI-COR Biosciences, Lincoln, NE). For infrared imaging, IRDye 680 conjugated goat anti-rabbit IgG (catalog number 926-32221, LI-COR Biosciences) and IRDye 800CW conjugated goat anti-mouse IgG (catalog number 926-32210, LI-COR Biosciences) were used instead of horseradish peroxidase-conjugated secondary antibodies. For quantification, values were normalized to appropriate loading controls.

Acetyl-CoA:Lysine Acetyltransferase Activity—For the analysis of the acetyltransferase activity, we employed affinity-purified BACE1 as acceptor of the acetyl group and [³H]acetyl-CoA as donor of the acetyl group. The acetyl-CoA:lysine acetyltransferases (ATase1 and/or ATase2) were provided either as pure enzymes following affinity purification with the ProFound kit

(see supplemental Methods) or as membrane extracts of stably transfected CHO cells. The reaction was performed in 150–200 μ l of acetylation buffer (50 mM Tris-HCl (pH 8.0), 0.1 mM EDTA, 1 mM dithiothreitol, 10% glycerol, 20 μ M acetyl-CoA) and let run for 1 h at 30 °C. The reaction was stopped by adding an equal volume of ice-cold buffer and immediate immersion in ice; BACE1 was immunoprecipitated with an anti BACE1 N-terminal monoclonal antibody and then counted on a liquid scintillation counter. The experimental controls are described in the appropriate figure legends.

Additionally, the acetyltransferase activity of affinity-purified ATase1 and ATase2 was assayed with commercially available colorimetric (catalog number K332-100, BioVision Inc.) and fluorescent kits (catalog number 10006515, Cayman Chemicals). The assays were performed as recommended by the manufacturer.

Real Time PCR—Total RNA from H4 (human neuroglioma) and SH-SY5Y (human neuroblastoma) cells was extracted and purified using the RNeasy plus mini kit (Qiagen). cDNA was synthesized using the SuperScript double-stranded cDNA synthesis system (Invitrogen) and then PCR-amplified. Primers used for RT-PCR were as follows: *GAPDH*, forward 5'-GAAGGTGAAGGTCGGAGTC-3', reverse 5'-GAAGATGGTGATGGGATTTTC-3'; *ATase1*, forward 5'-CGATTACTGAAGCTGCCTCGA-3', reverse 5'-GGTTTTTTGGCAAGGAACCA-C-3'; and *ATase2*, forward 5'-TCCTTGCCAAAAACCCTGG-3', reverse 5'-ATGCCACCACCTTCTCTTCA-3'. RNA quantification was performed by real time PCR in a ABI PRISM 7000 sequence detection system using SYBR Green PCR master mix (Applied Biosystems). Amplifications were generated at 2 min at 52 °C and 3 min at 95 °C, followed by 40 cycles of denaturations at 95 °C for 15 s, annealing, and synthesis (30 s at 61 °C and 30 s at 72 °C). $\Delta\Delta C_t$ values (14) were normalized with those obtained from the amplification of GAPDH and were expressed as fold-change over control. The assay was repeated three times, with each assay containing triplicate reactions and with each assay including an independent amplification of the probes.

Statistical Analysis—Results are always expressed as mean \pm S.D. of the indicated number of determinations. The data were analyzed by analysis of variance and Student's *t* test comparison, using GraphPad InStat3 software. Statistical significance was reached at *p* < 0.05.

RESULTS

Identification of ATase1 and ATase2 as Two Putative ER/ERGIC Acetyl-CoA:Lysine Acetyltransferases—Our studies previously demonstrated the presence of acetyl-CoA:lysine acetyltransferase activity in the ER/ERGIC. They also demonstrated that the catalytic site of the putative ER/ERGIC-based acetyltransferase(s) faced the lumen of the organelle (5). To identify the corresponding gene(s), we searched in the human genome for proteins displaying structural similarities to the histone acetyltransferase catalytic domain. The search yielded 46 possible candidates, 2 of which were predicted to function in the ER/ERGIC. The candidates had unknown biochemical function and were initially named Camello-like 2 (accession number NM_016347; also called putative *N*-acetyltransferase 8B) and Camello-like 1 (accession number NM_003960; also called

ATase1 and ATase2 Acetylate Nascent BACE1

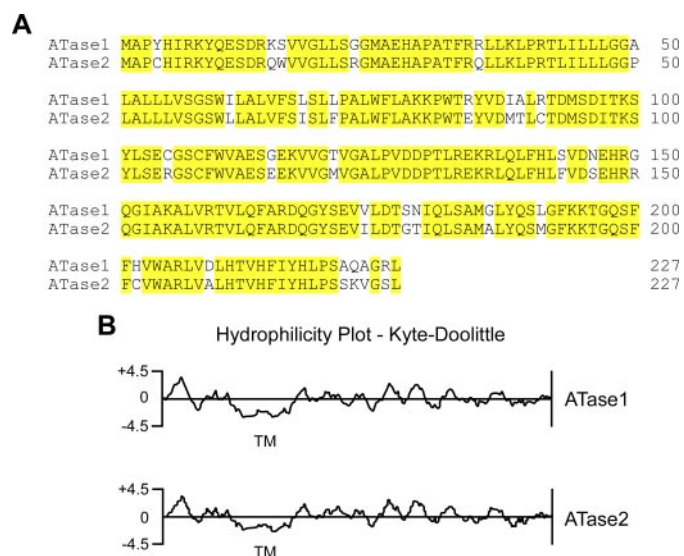


FIGURE 1. Schematic view of ATase1 and ATase2. A, alignment of amino acid sequences of ATase1 and ATase2. Alignment was performed by using the Megalign component of the DNASTAR (Lasergene version 6) software on a basis of ClustalW algorithm. Identical amino acids are highlighted in yellow. B, hydrophilicity profile (Kyte-Doolittle algorithm) of ATase1 and ATase2 was calculated using the protean component of the DNASTAR (Lasergene version 6) software. *TM* indicates the transmembrane (hydrophobic) domain.

putative *N*-acetyltransferase 8). They appear to have orthologs in *Xenopus laevis* (15) but not in *Caenorhabditis elegans* or *Drosophila melanogaster*.

The biochemical activity of both proteins was explored, and based on the results reported here they were re-named acetyltransferase 1 (ATase1) and 2 (ATase2) to indicate their biochemical function rather than the domain organization. Both ATase1 and ATase2 have a high probability of being ER/ERGIC-resident proteins (*k*-NN prediction using the PSORT II software of the University of Tokyo, Japan and available on line) (16, 17). Alignment of the amino acid sequences of ATase1 and ATase2 reveals an 88% sequence identity between the two proteins (Fig. 1A); the Kyte-Doolittle hydrophilicity/hydrophobicity plot (Fig. 1B) indicates the presence of one single hydrophobic segment, corresponding to the membrane-spanning domain. In both cases the putative catalytic site is situated in the C-terminal domain and is predicted to face the lumen of the ER/ERGIC.

ATase1 Is an ER/ERGIC Resident Acetyl-CoA:Lysine Acetyltransferase—We initially targeted ATase1, which was cloned and inserted into a mammalian expression vector containing a Myc tag at the C terminus, to allow subcellular localization and affinity purification for the *in vitro* studies. Stable transfection in CHO cells yielded several colonies overexpressing ATase1 (Fig. 2A). Membrane extracts from nontransfected control and ATase1-expressing cells were analyzed *in vitro* for acetyl-CoA:lysine acetyltransferase activity. The assay was performed in the presence of affinity-purified BACE1, which served as acceptor of the acetyl group, and radiolabeled acetyl-CoA, which served as donor of the acetyl group. Fig. 2B shows that the expression of ATase1 increased the acetyltransferase activity recovered from membrane extracts by ~2-fold. No activity was observed when the assay was performed in the absence of extracts (source of the enzymatic activity) or in the

presence of extracts that had been boiled prior to the incubation (Fig. 2B).

Subcellular fractionation studies indicated a predominant ERGIC localization that extended to ER, but not to Golgi, fractions (Fig. 2C), which is consistent with our previous localization of the ER/ERGIC-based acetyl-CoA:lysine acetyltransferase activity (5). The subcellular localization of ATase1 overlaps with the compartments where the acetylation of nascent BACE1 occurs and the nonacetylated mutants of BACE1 are retained (5). In fact, we have previously demonstrated that the Lys-to-Ala (BACE1_{Ala}) and the Lys-to-Arg (BACE1_{Arg}) mutant forms of BACE1 cannot be acetylated *in vivo* and *in vitro*, are retained in the ER/ERGIC system, and rapidly degraded by a proteasome-independent system (5, 6). Next, we analyzed the acetyl-CoA:lysine acetyltransferase activity of the individual fractions from the gradient shown in Fig. 2C and found that the distribution pattern of ATase1 completely overlapped with the acetyl-CoA:lysine acetyltransferase activity (Fig. 2D). Finally, when compared with control (nontransfected) cells, ERGIC fractions from ATase1-expressing cells displayed increased (~2-fold) acetyltransferase activity (Fig. 2E).

The above results indicate that ATase1 is localized in the compartments where the acetylation of nascent BACE1 normally occurs. They also indicate that the overexpression of ATase1 results in increased acetyl-CoA:lysine acetyltransferase activity. However, they do not rule out the possibility that ATase1 is only a co-factor in the reaction of lysine acetylation. To address this issue, we used affinity-purified ATase1 (instead of membrane extracts) for the *in vitro* acetylation of BACE1. As control, we used BACE1_{Arg}, which does not act as acceptor of the acetyl groups *in vitro* or *in vivo* (5). Fig. 3A shows that purified ATase1 was able to acetylate BACE1_{WT} but not BACE1_{Arg} proving that it is an acetyl-CoA:lysine acetyltransferase. The results obtained with BACE1_{Arg} are particularly important because they indicate that ATase1 can only acetylate the lysine residues that are found acetylated under physiological conditions (5).

Next, we incubated ATase1 with BACE1 in the presence of nonradiolabeled acetyl-CoA. Both BACE1 and ATase1 were purified by affinity chromatography prior to the incubation. BACE1 was then immunoprecipitated at the end of the reaction and analyzed by classical immunoblotting. In the absence of ATase1 only the immature form of BACE1 could be detected with an anti-acetylated lysine antibody (Fig. 3B, left panel, -ATase1, indicated by 1). However, incubation with ATase1 allowed detection of two additional bands corresponding to the fully mature and a biosynthetic intermediate form of BACE1 (Fig. 3B, left panel, +ATase1, indicated by 2 and 3). These results confirm those performed with radiolabeled acetyl-CoA (Fig. 3A) and clearly indicate that ATase1 can acetylate BACE1. The normal migration of the mature and biosynthetic intermediate forms of BACE1 is shown in the middle panel of Fig. 3B and in supplemental Fig. 1. The anti-acetylated lysine antibody also detected a lower band migrating with the predicted molecular mass of the cleaved ectodomain of BACE1 (Fig. 3B, left panel, indicated by *). The same band could be detected with an antibody against the N-terminal domain of BACE1 (data not shown) but not with antibodies raised against the C-terminal

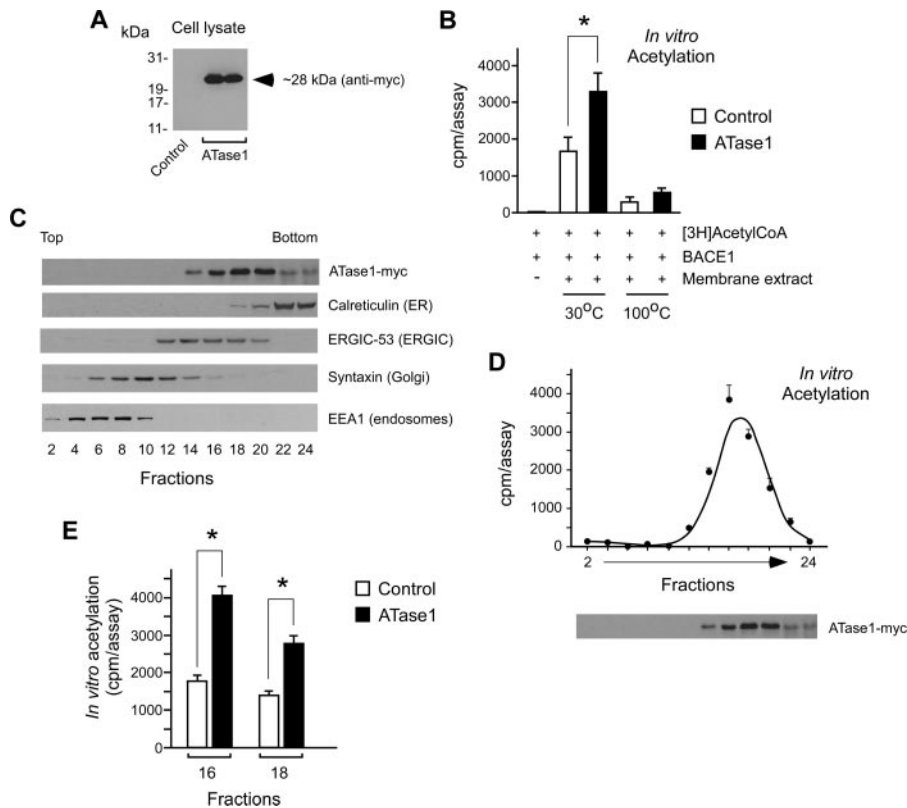


FIGURE 2. ATase1 is localized in the early secretory pathway and has acetyl-CoA:lysine acetyltransferase activity. *A*, Western blot analysis of control (nontransfected) and ATase1-expressing CHO cells. ATase1 migrates with the expected mass on SDS-PAGE. *B*, total membrane extract from control and ATase1-expressing cells was incubated with [³H]acetyl-CoA and affinity-purified BACE1 for 1 h at 30 °C. Reaction was stopped by lowering the temperature; BACE1 was then purified again and analyzed on a scintillation liquid counter. As control, BACE1 was also incubated with [³H]acetyl-CoA in the absence of membrane extracts and with a membrane extract that had been boiled for 10 min prior to the reaction. Results are the average ($n = 6$) \pm S.D. Asterisk indicates statistical significance ($p < 0.005$). *C*, subcellular distribution of ATase1 was analyzed by SDS-PAGE and immunoblotting after separation of intracellular membranes on a 10–24% discontinuous Nycodenz gradient. The appropriate subcellular markers are indicated. *D*, fractions shown in *C* were assayed for acetyl-CoA:lysine acetyltransferase activity as described in *B*. [³H]Acetyl-CoA served as donor of the acetyl group, whereas affinity-purified BACE1 served as acceptor substrate. Results are the average ($n = 3$) \pm S.D. The migration pattern of ATase1 shown in *C* is shown here again to allow comparison with the biochemical activity of the single fractions. *E*, fraction 16 and 18 of a subcellular fractionation gradient (see *C*) from control and ATase1-expressing cells were compared for acetyl-CoA:lysine acetyltransferase activity. The assay was run as in *D*. Results are the average ($n = 3$) \pm S.D. Asterisk indicates statistical significance ($p < 0.005$).

domain of BACE1 or the Myc tag (Fig. 3*B*, middle and right panels, indicated by *). The band was never observed immediately after purification of BACE1 and appeared only after the 6-h incubation required for the *in vitro* acetylation assay, suggesting that it corresponds to the cleaved N-terminal ectodomain of BACE1 and most likely results from *in vitro* autocatalytic cleavage, as described previously (18).

Surprisingly, the anti-acetylated lysine antibody recognized a band of ~28 kDa, which corresponds to ATase1 (Fig. 3*B*, left panel, +ATase1). In fact, the same band could be observed with anti-Myc antibodies (Fig. 3*B*, right panel, +ATase1) but not with antibodies against the N-terminal (data not shown) or C-terminal domain (Fig. 3*B*, middle panel) of BACE1. Therefore, these results indicate that ATase1 can interact with BACE1 *in vitro* and can undergo acetylation in one or more lysine residues, most likely through an autocatalytic mechanism (discussed below).

ATase2 Is an ER/ERGIC Resident Acetyl-CoA:Lysine Acetyltransferase—We next cloned ATase2 into a mammalian expression vector containing a Myc tag at the C terminus. This

construct was used to generate cells stably expressing ATase2 and ATase1 + ATase2 (Fig. 4*A*). Similarly to ATase1, the expression of ATase2 alone increased (by ~3-fold) the acetyl-CoA:lysine acetyltransferase activity recovered from total membrane extracts (Fig. 4*B*). In addition, the subcellular distribution of ATase2 (Fig. 4*C*), even though slightly different, appeared to overlap with ATase1 (Fig. 2*C*) and with the normal distribution of the acetyl-CoA:lysine acetyltransferase activity (Fig. 2*D*). Finally, ER/ERGIC fractions generated from ATase2-expressing cells displayed increased acetyltransferase activity, when compared with corresponding fractions from control nontransfected cells (Fig. 4*D*). As with ATase1-expressing cells (Fig. 2*D*), no activity was found in fractions corresponding to the Golgi apparatus (data not shown, see also Ref. 5).

When affinity-purified ATase2 was incubated with BACE1 and nonradiolabeled acetyl-CoA, we found a marked increase in the acetylation of both biosynthetic intermediates of BACE1 (Fig. 5*A*, left panel). Interestingly, the acetylation pattern produced by ATase2 seems somehow different from the one observed with ATase1 (compare Fig. 5*A* to Fig. 3*B*) suggesting potential differences in substrate recognition activities of the two enzymes. Similarly to ATase1, the immunoprecipitation of BACE1 resulted in the pulldown of ATase2, suggesting physical interaction, at least *in vitro* (Fig. 5*A*, right panel). However, in contrast to ATase1, we could not clearly resolve a band corresponding to ATase2 with an anti-acetylated lysine antibody (Fig. 5*A*, left panel). This occurred even though ATase2 could clearly be identified with an anti-Myc antibody (Fig. 5*A*, right panel). These results might indicate potential differences in the biochemical properties and functional regulation of ATase1 and ATase2 (discussed below). Finally, incubation of ATase2 with BACE1 and radiolabeled acetyl-CoA resulted in acetylation of BACE1_{WT} but not BACE1_{Arg} (Fig. 5*B*) proving that ATase2 can only acetylate the lysine residues that are found acetylated under physiological conditions (5).

We next used a commercially available colorimetric assay that employs a recombinant peptide corresponding to the N-terminal tail of the histone protein, as acceptor of the acetyl group, and a highly concentrated nuclear histone acetyltransferase (HAT) preparation, as enzyme. The assay was partially modified to employ our affinity-purified ATases, instead of

ATase1 and ATase2 Acetylate Nascent BACE1

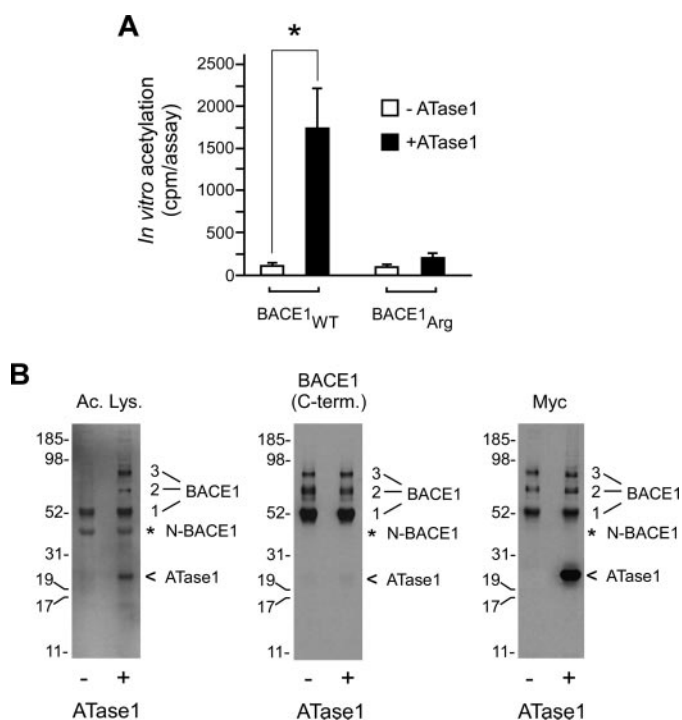


FIGURE 3. ATase1 acetylates BACE1 *in vitro*. *A*, affinity-purified ATase1 and BACE1 were co-incubated in the presence of [3 H]Acetyl-CoA for 1 h at 30 °C. Reaction was stopped by lowering the temperature; BACE1 was then purified again and analyzed on a scintillation liquid counter. The same assay was repeated with BACE1_{Arg}, a mutant form of BACE1 where the lysine residues that serve as acceptors of the acetyl groups have been mutated to arginine (5). Results are the average ($n = 6$) \pm S.D. Asterisk indicates statistical significance ($p < 0.005$). *B*, affinity-purified ATase1 and BACE1 were co-incubated in the presence of acetyl-CoA (50 μ M) for 6 h at 30 °C. Reaction was stopped by lowering the temperature. BACE1 was then immunoprecipitated with a biobead cross-linked antibody specific for the N-terminal domain of BACE1 and analyzed by Western blotting with the indicated antibodies (Ac. Lys., anti-acetylated lysine; BACE1 C-term., anti-BACE1 C-terminal domain; Myc, anti-Myc). Numbers indicate the different species of BACE1 (see supplemental Fig. 1 for detailed explanation). Asterisk indicates a band that could be recognized with an antibody against the N-terminal domain of BACE1 and migrated with the expected molecular mass of the cleaved ectodomain of BACE1. < indicates ATase1.

HAT, as source of the enzymatic activity. Fig. 5C shows that both ATase1 and ATase2 displayed robust acetyl-CoA:lysine acetyltransferase activity, which was in the same range of that observed with HAT. Finally, when ATase1 and ATase2 were included together in the assay, we detected a clear additive effect indicating that the two enzymes can act independently of each other, at least *in vitro*. It remains to be determined whether the additive effect is caused by their ability to target different lysine residues of the substrate-peptide or by the presence of excess substrate in the assay. The ability of ATase1 and ATase2 to acetylate an appropriate substrate was also confirmed by using a fluorescent assay that employs the histone H3-(5–23) peptide as acceptor and acetyl-CoA as donor (supplemental Fig. 2).

Catalytic C-terminal Domain of ATase1 and ATase2 Faces the Lumen of the ER/ERGIC System—We have previously shown that the transient acetylation of the N-terminal and globular domain of nascent BACE1 occurs in the lumen of the ER/ERGIC system (5). We also demonstrated that the acetyltransferase activity responsible for the lysine acetylation of the nascent protein was positioned in the luminal face of the secre-

tory compartment (5). The hydrophilic/hydrophobic plot (Fig. 1B) together with the apparent topology (using the MTOP prediction model (19)) of ATase1 and ATase2 predicts the C-terminal domain, which contains the acetyl-CoA:lysine acetyltransferase homology domain, to face the lumen of the ER/ERGIC system.

We decided to assess whether this was indeed the case by assaying *in vitro* the acetyl-CoA:lysine acetyltransferase activity recovered from ERGIC vesicles of ATase1- or ATase2-expressing cells under two different experimental conditions as follows: in the presence or absence of mild concentrations (0.2–0.5%) of Triton X-100 (Fig. 6A). When prepared, vesicles are sealed and of the same membrane topographical orientation as *in vivo* (5, 20–22). Therefore, under normal conditions (Fig. 6A, *Sealed*) the acetylation of affinity-purified BACE1 can occur only if the catalytic site of the enzyme (ATase1 or ATase2) is facing the outside/cytosolic face of the vesicles. Conversely, if the catalytic site of the enzyme resides in the luminal face of the vesicles, the reaction will only occur in the presence of mild concentrations of detergent, which will allow access of both the acceptor (purified BACE1) and donor (radiolabeled acetyl-CoA) to ATase1 or ATase2 (Fig. 6A, *Opened*). Fig. 6B clearly shows that the acetyltransferase activity of native ATase1 and ATase2 could only be observed in the presence of Triton X-100, indicating that the catalytic site is facing the lumen of the organelle in its native conditions. The activity recovered in the absence of Triton X-100 was in the normal range of latency (3–5%) observed with the glucose-6-phosphatase and sialyltransferase methods (see supplemental Methods).

Next, we took advantage of the fact that both ATase1 and ATase2 have a Myc tag at the C terminus, which is predicted to face the lumen of the ER/ERGIC system. Therefore, the above vesicles were incubated with an anti-Myc antibody covalently attached to aldehyde-activated agarose beads (ProFound system) for immunoprecipitation. The experiment was performed under both the “opened” and “sealed” conditions (Fig. 6A) to determine the topology of the enzymes. Fig. 6C shows that ATase1 and ATase2 could be immunoprecipitated only when the vesicles were used under the opened condition, which allowed the anti-Myc antibody to interact with the C-terminal Myc tag. Therefore, when taken together, the above results indicate that both ATase1 and ATase2 have the predicted topology, with the catalytic C-terminal domain facing the lumen of the ER/ERGIC system, where the lysine acetylation of nascent BACE1 normally occurs.

ATase1 and ATase2 Influence the Steady-state Levels of BACE1 and the Generation of A β —The results shown in Figs. 3B and 5A indicate that both ATase1 and ATase2 can be co-immunoprecipitated with BACE1 suggesting physical interaction. However, this experiment was performed after co-incubation of affinity-purified ATases and BACE1 *in vitro*. Therefore, we decided to assess whether the physical interaction between the enzyme (ATases) and the substrate (BACE1) also occurred *in vivo*. For this experiment we used cell lines that had been transfected with ATase1-myc or ATase2-myc, but not with BACE1-myc, so that we could clearly analyze the possible interaction with endogenous BACE1. ATase1 and ATase2 were purified (Fig. 7A, *upper panel*) with the anti-Myc-aldehyde-ac-

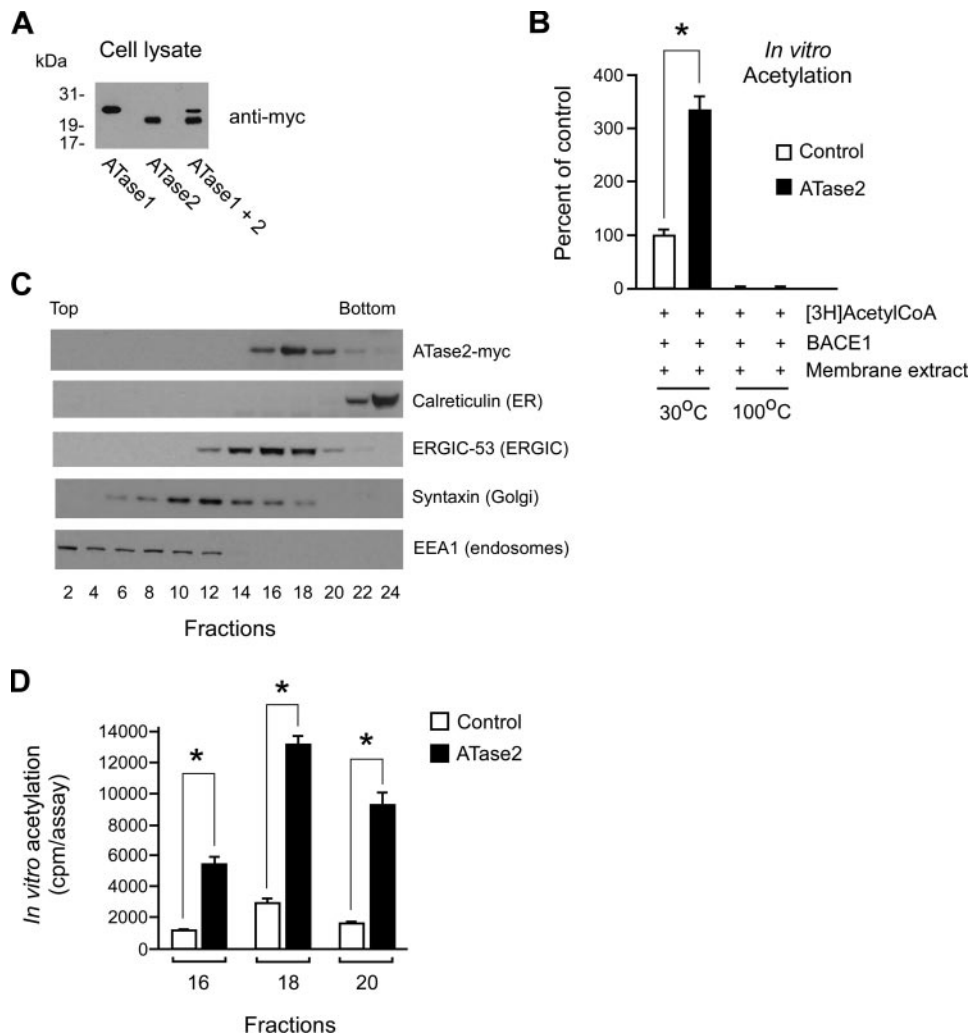


FIGURE 4. ATase2 is localized in the early secretory pathway and has acetyl-CoA:lysine acetyltransferase activity. *A*, Western blot analysis of ATase1, ATase2, and ATase1 + 2 expressing CHO cells. *B*, total membrane extract from control (nontransfected) and ATase2-expressing cells was assayed for acetyltransferase activity as in Fig. 2*B*. Results are expressed as percent of control and are the average ($n = 6$) \pm S.D. Asterisk indicates statistical significance ($p < 0.005$). *C*, subcellular distribution of ATase2 was analyzed by SDS-PAGE and immunoblotting after separation of intracellular membranes on a 10–24% discontinuous Nycodenz gradient. The appropriate subcellular markers are indicated. *D*, fractions 16, 18, and 20 of a subcellular fractionation gradient (see *C*) from control and ATase2-expressing cells were compared for acetyl-CoA:lysine acetyltransferase activity. The assay was performed as in Fig. 2*E*. Results are the average ($n = 6$) \pm S.D. Asterisk indicates statistical significance ($p < 0.005$).

tivated agarose beads (ProFound system) employed in Fig. 6*C* and then analyzed by immunoblotting with an anti-BACE1 antibody. Fig. 7*A* (middle panel, anti-BACE1) clearly shows that BACE1 was present in the immunoprecipitate indicating that both acetyltransferases interact with endogenous BACE1 *in vivo*. Importantly, only the two lower bands corresponding to biosynthetic intermediates of BACE1 (Fig. 7*A*, compare the middle panel with the normal migration pattern of affinity-purified BACE1 on a similar SDS-PAGE system, shown in Figs. 3*B* and 5*A*) could be co-immunopurified with ATase1 and ATase2 (see also supplemental Fig. 1). These results are perfectly consistent with the fact that ATase1 and ATase2 are localized in the ER and ERGIC (Figs. 2*C* and 4*C*), where both biosynthetic intermediates of BACE1 can be found (supplemental Fig. 1*A*; see also Ref. 5). However, they are also surprising because we initially thought that only the lower species,

migrating at ~52–55 kDa, was acetylated. In fact, the ~52–55-kDa band is the only one that can be detected with anti-acetylated lysine antibodies after immunoprecipitation of BACE1 from cell lysates (5) (see also Fig. 7*D*). This apparent discrepancy could be caused by the low levels and rapid metabolism of the upper biosynthetic intermediate that migrates at ~65 kDa (see also Fig. 7*E*). In fact the detection of this species is enhanced by subcellular fractionation (see supplemental Fig. 1*A*) or affinity purification (see Figs. 3*B* and 5*A*). To address this issue, we analyzed the acetylation pattern of BACE1 after immunopurification of ATase1 and ATase2. Fig. 7*A* (lower panel, anti-Ac. Lys.) clearly shows that both BACE1 biosynthetic intermediates are acetylated. Therefore, when taken together, these results indicate that ATase1 and ATase2 interact with nascent BACE1 in the ER/ERGIC system (see also supplemental Fig. 1*B* for a schematic overview).

We previously published that the lysine acetylation of nascent BACE1 results in molecular stabilization and increased steady-state levels of the β -secretase (5). Therefore, we analyzed whether the overexpression of ATase1 and ATase2 affected the levels of BACE1 and/or the production of $A\beta$. The results shown in Fig. 7*B* indicate that both ATase1 and ATase2 caused an increase in the steady-state levels of endogenous BACE1, with ATase2 displaying an apparent stronger effect, which could be related to the more powerful acetyl-CoA:lysine acetyltransferase activity observed *in vitro* (compare Fig. 4*B* with Fig. 2*B* for total membrane extracts and Fig. 4*D* with Fig. 2*E* for the individual fractions). These results were supported by the increased levels of $A\beta$ secreted in the conditioned media (Fig. 7*C*), by the increased levels of endogenous C99 (supplemental Fig. 3), and by the apparent increase in the lysine acetylation of endogenous BACE1 (Fig. 7*D*) in ATase1- and ATase2-expressing cells. C99 is the C-terminal fragment of APP that results from BACE1-mediated cleavage of APP and represents the immediate substrate for the generation of $A\beta$.

The detection of the acetylated intermediates of nascent BACE1 from total cell lysates is normally hampered by the rapid deacetylation that occurs in the Golgi apparatus (5). To circumvent this obstacle, we also decided to immunoprecipitate BACE1 from ER/ERGIC vesicles prior to immunoblotting with

ATase1 and ATase2 Acetylate Nascent BACE1

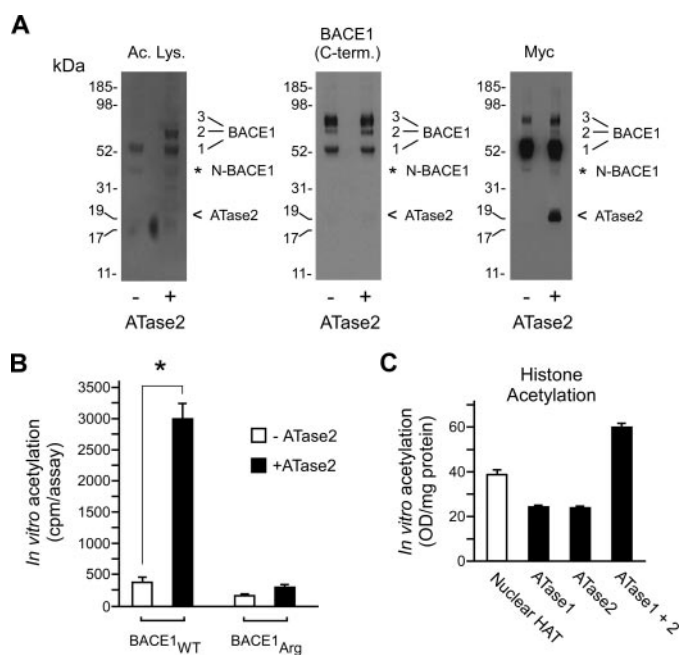


FIGURE 5. ATase2 acetylates BACE1 *in vitro*. *A*, affinity-purified ATase2 and BACE1 were co-incubated in the presence of acetyl-CoA (50 μ M) for 6 h at 30 °C. This experiment was performed as in Fig. 3*B*. Following immunoprecipitation with a bio-bead cross-linked antibody specific for the N-terminal domain, BACE1 was analyzed by SDS-PAGE and Western blotting. The following antibodies were used: *Ac. Lys.*, anti-acetylated lysine; *BACE1 C-term.*, anti-BACE1 C-terminal domain; *Myc*, anti-Myc. Numbers indicate the fully mature and biosynthetic intermediates of BACE1. Asterisk indicates a band that could be recognized with an antibody against the N-terminal domain of BACE1 and migrated with the expected molecular mass of the cleaved ectodomain of BACE1. < indicates ATase2. *B*, ATase2 was incubated with BACE1 in the presence of [³H]acetyl-CoA for 1 h at 30 °C as in Fig. 3*A*. Both the enzyme (ATase2) and the acceptor substrate (BACE1) were purified by affinity chromatography prior to the incubation. BACE1_{Arg} was used as control because the lysine residues that serve as acceptors of the acetyl groups have been mutated to arginine (5). Results are the average ($n = 6$) \pm S.D. Asterisk indicates statistical significance ($p < 0.005$). *C*, acetyl-CoA:lysine acetyltransferase activity of ATase1 and ATase2 was assayed with a commercially available colorimetric assay employing a pool of histone-tail-peptides as acceptor of the acetyl group. Both ATase1 and ATase2 were purified by affinity chromatography prior to the reaction. The acetyl-CoA:lysine acetyltransferase activity of a highly purified pool of nuclear HAT is also shown. Results are the average ($n = 3$) \pm S.D.

an anti-acetylated lysine antibody. Fig. 7*F* clearly shows that under the above conditions the detection of BACE1-acetylated intermediates is enhanced, and the effect caused by the overexpression of ATase1 and ATase2 is much more evident. In fact, both acetyltransferases caused a marked increase in the acetylation of the immature form of endogenous BACE1.

Next, we decided to down-regulate ATase1 and ATase2 and assess the effects on the steady-state levels of BACE1. Fig. 8, *A–C*, shows that two different siRNAs targeting ATase1 successfully reduced the steady-state levels of endogenous BACE1. Interestingly, the effects observed on the levels of BACE1 were proportional to the degree of ATase1 down-regulation induced by the different oligonucleotides. The fact that the down-regulation of ATase1 resulted in a marked reduction of endogenous BACE1 also indicates that ATase2 cannot replace the activity of ATase1 *in vivo*. It is worth stressing that the siRNA against ATase1 did not affect the expression of ATase2 (or vice versa; data not shown). This conclusion is consistent with the results shown in Fig. 5*C*, which indicate that ATase1 and ATase2 act as

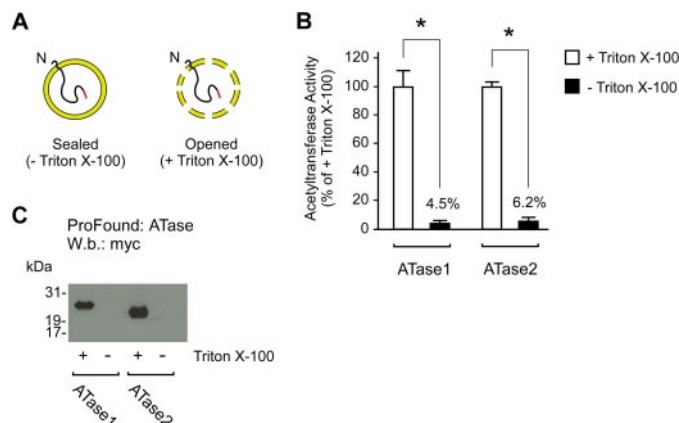


FIGURE 6. The C-terminal and catalytically active domains of ATase1 and ATase2 face the lumen of the ER/ERGIC. *A*, schematic view of the rationale of the experiments reported here (described under “Results”). The N terminus of either ATase1 or ATase2 is indicated. The C-terminal Myc tag is in red. *B*, ER and ERGIC vesicles from ATase1- and ATase2-expressing cells were incubated with affinity-purified BACE1 and [³H]acetyl-CoA for 1 h at 30 °C. Reaction was stopped by lowering the temperature; BACE1 was then purified again and analyzed on a scintillation liquid counter. Vesicles were used under the sealed (no detergent; black bars) or opened (+ detergent; white bars) condition. Results are expressed as percent of BACE1 acetylation obtained in the presence of detergent (opened condition) and are the average ($n = 6$) \pm S.D. Numbers on top of the black bars indicate the percent of total acetyl-CoA:lysine acetyltransferase activity recovered in the absence of detergent (sealed condition). *C*, sealed and opened vesicles shown in *A* were incubated with an anti-Myc antibody covalently attached to aldehyde-activated agarose beads (ProFound system) for immunoprecipitation. After extensive washing, bound proteins were eluted by lowering the pH and analyzed by SDS-PAGE and immunoblotting.

independent enzymes *in vitro*. The down-regulation of ATase2 also resulted in a modest decrease of BACE1 levels (Fig. 8, *D–F*). However, it is important to point out that the down-regulation of ATase2 was often accompanied by macroscopic cell death, which interfered with the analysis of BACE1 metabolism. Such an effect was independent of the transfection procedures and was never observed following down-regulation of ATase1 or other unrelated genes. Therefore, we interpret this as evidence of an important biological function of ATase2 in the cell. The down-regulation of ATase1 or ATase2 was also accompanied by decreased secretion of A β into the conditioned media (Fig. 8*G*) and by decreased levels of endogenous C99 (Fig. 8, *B* and *E*).

When taken together, the above results indicate that ATase1 and ATase2 influence the levels of BACE1 and the rate of A β generation. The results obtained with ATase1 and ATase2 siRNAs are particularly important because they indicate that biochemical inhibition of ATase1 and ATase2 might be useful for pharmacological approaches aimed at the prevention of late-onset AD.

Lipid Second Messenger Ceramide Increases the Levels of Endogenous ATase1 and ATase2—We previously published that ceramide treatment of different cell lines results in increased acetylation and stabilization of BACE1 (5, 7, 8). We also published that the increased activation of ceramide in the brain caused by either normal aging in wild-type mice or by the hyperactivation of IGF-1R signaling in p44^{+/+} transgenic mice, a model of accelerated aging (23), results in increased acetylation and stabilization of BACE1 (8, 9). Therefore, we decided to analyze the effects induced by ceramide on the mRNA levels of ATase1 and ATase2 in H4 (human neuroglioma) and SH-SY5Y

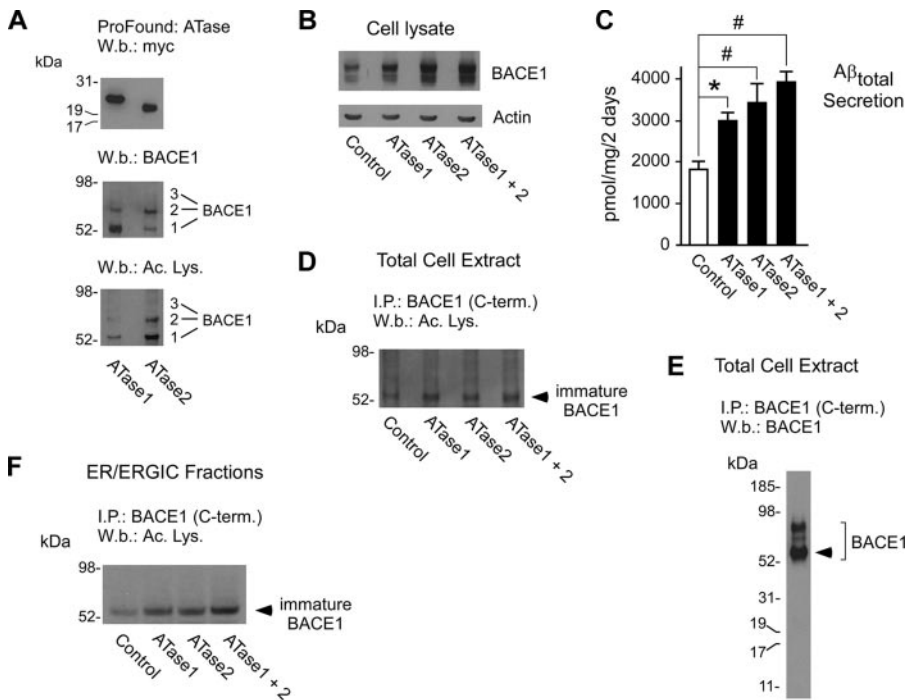


FIGURE 7. Overexpression of ATase1 and ATase2 increases the levels of BACE1 and the generation of Aβ. A, ATase1 and ATase2 were purified from stable-transfected cells with an anti-Myc antibody covalently attached to aldehyde-activated agarose beads (ProFound system) and then analyzed by Western blotting (*Web.*). The blot with anti-Myc (*upper panel*) demonstrates the presence of ATase1 and ATase2 in the immunoprecipitate, whereas the blot with anti-BACE1 (*middle panel*) shows the presence of endogenous BACE1. Finally, the blot with anti-acetylated lysine (*Ac. Lys.*; *lower panel*) shows the acetylation pattern of co-immunoprecipitated BACE1. The bands visible with the anti-BACE1 antibody correspond to biosynthetic intermediates of nascent BACE1 (see also supplemental Fig. 1A). The migration of the different forms of affinity-purified BACE1 on a similar SDS-PAGE system is shown in Figs. 3B and 5A. B, steady-state levels of endogenous BACE1 in ATase1-, ATase2-, and ATase1 + 2-expressing cells were analyzed by immunoblotting of total cell lysates. C, Aβ levels in the conditioned media were determined by standard sandwich enzyme-linked immunosorbent assay. Results are the average ($n = 3$) ± S.D. Symbols indicate statistical significance (*, $p < 0.05$; catalog number, $p < 0.005$). D, endogenous BACE1 was immunoprecipitated (*i.p.*) from total cell lysates of ATase1-, ATase2-, and ATase1 + 2-expressing cells prior to Western blot analysis with an anti-acetylated lysine antibody. As expected (5), only the ~52–55-kDa band corresponding to immature BACE1 could be visualized with an anti-acetylated lysine antibody. The migration of the different forms of BACE1 on a similar SDS-PAGE system is also shown for comparison (E). F, experiment described in D was repeated after immunoprecipitation of endogenous BACE1 from a pool of ER/ERGIC fractions (representative gradients are shown in Fig. 2C, Fig. 4C, and in supplemental Fig. 1).

(human neuroblastoma) cells. Under basal conditions the mRNA levels of both ATases were higher in SH-SY5Y than in H4 cells, suggesting possible cell-type differences (data not shown). However, when treated with ceramide, both cell lines displayed a marked activation of transcription of ATase1 and ATase2, as detected by quantitative real time PCR (Fig. 9). The effect could be observed as early as 4 h after treatment and was still evident after 4 days, which is consistent with the time course that we initially described (7, 8). In conclusion, the above results clearly demonstrate that ATase1 and ATase2 are up-regulated by ceramide treatment and suggest a possible implication in AD pathogenesis. In fact, AD patients have increased levels of ceramide (more than 3-fold, when compared with age-matched controls) in the brain (24, 25).

DISCUSSION

We have recently described a novel form of post-translational regulation of nascent BACE1 that involves transient acetylation of seven lysine residues in the lumen of the ER/ERGIC system followed by deacetylation of the mature protein in the

lumen of the Golgi apparatus (5). The acetylated protein is able to proceed along the secretory pathway and achieve conformational maturation/stability, whereas the nonacetylated intermediates are retained and disposed in the ERGIC (5). Being a novel form of post-translational regulation, the biochemical machinery responsible for these events is unknown. Here we report the identification of two ER/ERGIC-based acetyl-CoA:lysine acetyltransferases that are directly involved in the lysine acetylation of nascent BACE1. The proteins, initially named Camello-like 1 and Camello-like 2 for their structural organization, have no previously identified biochemical activity and were named here ATase1 and ATase2 to indicate their function.

Both ATase1 and ATase2 were shown to have acetyl-CoA:lysine acetyltransferase activity *in vitro* and under native conditions, and to be able to acetylate BACE1 in the lysine residues that we previously identified (5). Both enzymes were found to localize in the compartments where the lysine acetylation of BACE1 normally occurs, displaying a perfect co-distribution with the endogenous ER/ERGIC acetyl-CoA:lysine acetyltransferase activity, and to have the required topographical arrangement with the catalytic site facing the lumen of the ER/ERGIC, as predicted by our previous results (5). Finally, they were shown to interact with BACE1 *in vitro* and *in vivo* and to affect the steady-state levels of their immediate substrate.

Although they are 88% identical at the amino acid level and share several biochemical features, ATase1 and ATase2 seem to display two important differences. First, ATase1 could recognize and acetylate the fully mature form of BACE1, at least *in vitro*, whereas ATase2 could not; second, ATase1 could be detected with an anti-acetylated lysine antibody, whereas ATase2 could not. The former might indicate differences in substrate recognition properties of the two enzymes, whereas the latter might suggest different catalytic mechanisms. These differences might become important when attempting to design biochemical inhibitors for pharmacological purposes (26). In this regard, it is important to point out that p300 HAT contains an “activation/regulatory loop” that undergoes autoacetylation and functions as an allosteric switch that regulates its own acetyltransferase activity; when hypoacetylated it inhibits, and when autoacetylated it activates the activity of the enzyme (27, 28). Therefore, it is possible that ATase1 can

ATase1 and ATase2 Acetylate Nascent BACE1

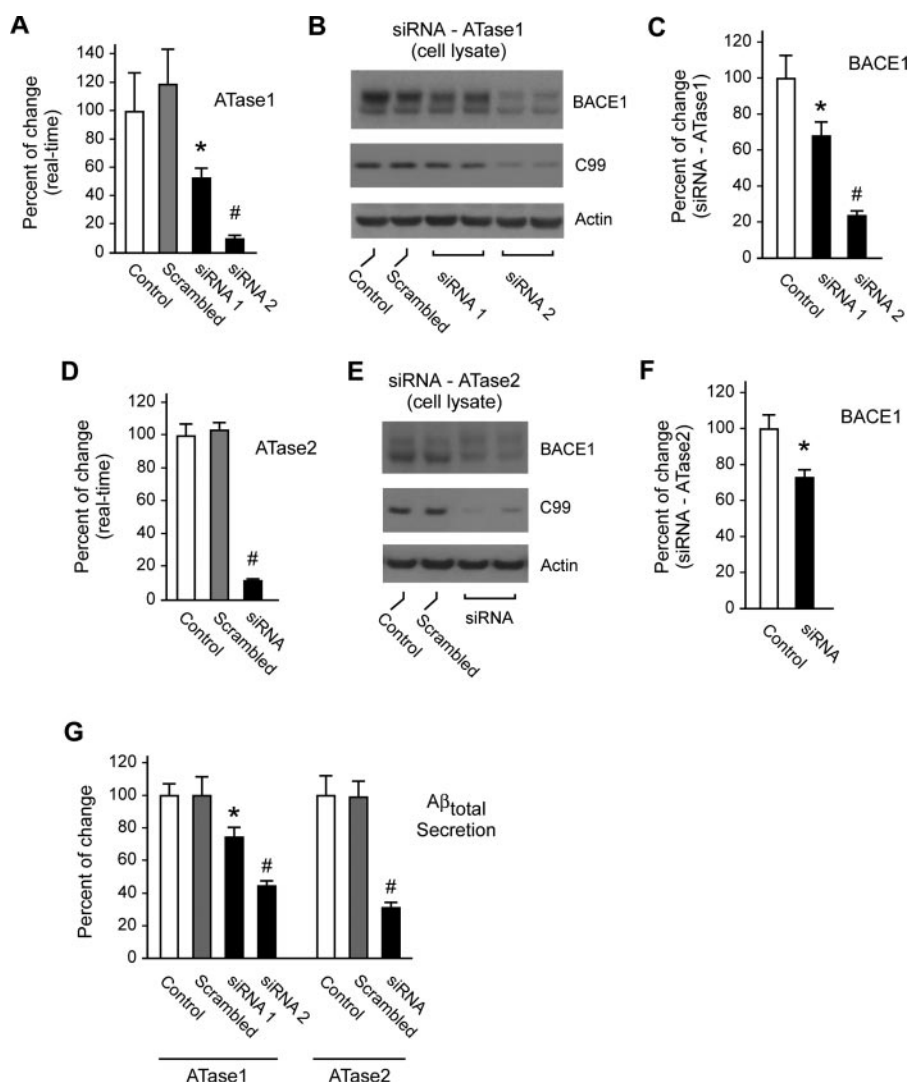


FIGURE 8. Down-regulation of ATase1 and ATase2 decreases the levels of BACE1 and the generation of A β . A–C, H4 (human neuroglioma) cells were treated with two different siRNAs targeting ATase1 prior to real time quantification of ATase1 mRNA levels (A) and Western blot analysis of BACE1 and C99 levels (B). The quantification of BACE1 protein changes after siRNA is shown in C. As control, cells were also treated with scrambled (nonsilencing) siRNA. D–F, H4 cells were treated with siRNA targeting ATase2 prior to real time quantification of ATase2 mRNA levels (D) and Western blot analysis of BACE1 and C99 levels (E). The quantification of BACE1 protein changes after siRNA is shown in F. As control, cells were also treated with scrambled (nonsilencing) siRNA. G, A β levels in the conditioned media of siRNA-treated cells were determined by standard sandwich enzyme-linked immunosorbent assay. Results are expressed as percent of control (no treatment) and are the average ($n = 6$) \pm S.D. Symbols indicate statistical significance (*, $p < 0.05$; catalog number, $p < 0.005$).

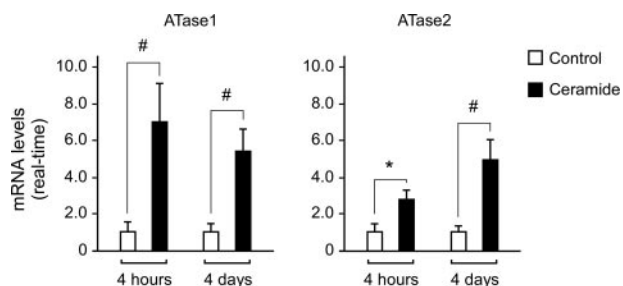


FIGURE 9. Ceramide treatment increases the levels of endogenous ATase1 and ATase2. SH-SY5Y cells were treated with ceramide ($10 \mu\text{M}$) for the indicated period of time prior to real time quantitative PCR. The 4-h treatment was performed in the presence of 0.5% fetal bovine serum, whereas the 4-day treatment was performed in the presence of 10% fetal bovine serum, as described previously (5, 7, 8). Results are expressed as fold ($n = 4$) \pm S.D. of control (no treatment). Symbols indicate statistical significance (*, $p < 0.05$; catalog number, $p < 0.005$). No difference was observed in the mRNA levels of GAPDH, which was used as internal control.

undergo autoacetylation and that this event might function as an allosteric mechanism to control its own biochemical activity. Considering that the down-regulation of ATase1 resulted in a dramatic decrease in the levels of endogenous BACE1 in the absence of evident cell death/toxicity, this particular enzymatic feature could serve to develop specific biochemical inhibitors.

The transient acetylation of the ϵ -amino group of a lysine residue has been traditionally associated with histone proteins, where it serves to control chromatin folding and DNA transcription, and cytoplasmic/nuclear proteins (mostly transcription factors), where it serves to regulate stability, activity, and protein-protein interactions (29–32). However, recently Schwer *et al.* reported (33) that a similar event regulates the activity of a mitochondrial-matrix enzyme, whereas we reported (5) that a transient form of lysine acetylation regulates the maturation, trafficking along the secretory pathway, and molecular stability of a nascent membrane protein. Therefore, this relatively new form of post-translational modification seems to perform different purposes in different organelles. It is worth noting that we recently identified a second membrane protein that undergoes transient acetylation in the early secretory pathway, the low density lipoprotein receptor (6).

Although the primary amino acid sequence contains the basic information to ensure correct folding of a

nascent membrane/secretory protein, the process is favored by transient or permanent post-translational modifications (1). The transient lysine acetylation of BACE1 seems to affect both the stability/half-life of the nascent protein and its ability to leave the early secretory pathway (5). The information obtained with the membrane protein BACE1 (reported here and in our previous publication (5)) indicates that different biochemical activities have been positioned in the secretory pathway to ensure acetylation and deacetylation of BACE1, and possibly other membrane/secretory proteins. It is worth mentioning that we are currently completing the biochemical characterization of an acetyl-CoA membrane transporter that is solely found in the ER. The transporter makes the donor of the acetyl group (acetyl-CoA) available for the reaction of acetylation and, therefore, is crucial for the activity of ATase1 and ATase2,

which are found in the ER/ERGIC system. Interestingly, ceramide regulates the steady-state levels of the transporter *in vivo* (data not shown) and, consequently, the efficiency of acetyl-CoA transport into the lumen of the ER (5). Finally, we previously reported that the deacetylase, which is responsible for removing the acetyl groups from nascent BACE1, is solely found in the Golgi apparatus (5). Therefore, when taken together, these results indicate that the different components of the acetylation/deacetylation machinery have been strategically inserted along the secretory pathway to ensure availability of the required substrate and enzymes and the correct sequence of the biochemical events.

The subcellular distribution profile of ATase1 and ATase2 shows a predominant ERGIC localization that extends to the ER but not to the Golgi apparatus (Fig. 2C, Fig. 4C, and supplemental Fig. 1). This is consistent with the fact that the immunopurification of ATase1 or ATase2 pulls down the two biosynthetic (acetylated) intermediates of BACE1 that are found in the ER/ERGIC system (Fig. 7A and supplemental Fig. 1). These results might suggest that the ATases act both as modifying enzymes (acetyltransferases) and chaperones of nascent BACE1. The fact that the lysine residues that are acetylated in BACE1 appear to be on the same face of the protein and to surround the catalytic pocket of the enzyme (5) suggests that the ATases “shield” nascent BACE1. Consistently with the above model, the “loss-of-acetylation” mutant versions of BACE1 are retained and degraded in the early secretory pathway by PCSK9/NARC-1 even though efficiently synthesized (5, 6). In contrast, the “gain-of-acetylation” mutant is protected from degradation in the early secretory pathway. Therefore, we could envision a mechanism in which a stoichiometric competition between the acetyltransferases and the ERGIC-based degrading machinery regulates the steady-state levels of BACE1; ATase-bound (acetylated) BACE1 would be protected from degradation whereas ATase-unbound (nonacetylated) BACE1 would not.

The Camello ortholog Xcml in *X. laevis* has been shown to regulate cell migration and adhesion very early in embryogenesis, during the process of gastrulation (15). The molecular mechanism, even though unexplored and unknown, appeared to involve some sort of protein modification (presumably acetylation) in the early secretory pathway (presumably in the lumen of the ER). Even though we now offer a clear biochemical function for the human Camello-like proteins ATase1 and ATase2, the findings reported by Popsueva *et al.* (15) point to a crucial role of these enzymes in basic cellular events such as cell migration, cell-cell interaction, and development. The cell toxicity observed following down-regulation of ATase2 seems to support this conclusion. Because post-translational modifications of membrane proteins in the ER and Golgi apparatus are crucial for the correct assembly and function of the mature proteins, it is not surprising that the enzymes involved in such modifications might be crucial themselves (1, 2, 34).

The fact that the events described here act downstream of the aging program mediated by IGF-1R, the common regulator of life span in all organisms (10, 35–37), in regulating the rate of A β generation (5, 7–9) suggests a possible implication in late-

onset AD neuropathology. This scenario would be supported by the fact that ceramide levels are higher in late-onset AD brains, when compared with age-matched controls (24, 25). Therefore, it is possible that the biochemical characterization of the acetylation/deacetylation machinery may lead to the identification of novel pharmacological strategies for the prevention of late-onset AD.

Acknowledgments—We thank Nansi Jo Colley and Gail Robertson for critical reading of an early version of this manuscript and the members of the Puglielli laboratory for critical discussion and comments. We also thank Dr. Robert Vassar for the BACE1-Cat1 antibody.

REFERENCES

1. Trombetta, E. S., and Parodi, A. J. (2003) *Annu. Rev. Cell Dev. Biol.* **19**, 649–676
2. Dempksi, R. E., Jr., and Imperiali, B. (2002) *Curr. Opin. Chem. Biol.* **6**, 844–850
3. Kleizen, B., and Braakman, I. (2004) *Curr. Opin. Cell Biol.* **16**, 343–349
4. Meusser, B., Hirsch, C., Jarosch, E., and Sommer, T. (2005) *Nat. Cell Biol.* **7**, 766–772
5. Costantini, C., Ko, M. H., Jonas, M. C., and Puglielli, L. (2007) *Biochem. J.* **407**, 383–395
6. Jonas, M. C., Costantini, C., and Puglielli, L. (2008) *EMBO Rep.* **9**, 916–922
7. Puglielli, L., Ellis, B. C., Saunders, A. J., and Kovacs, D. M. (2003) *J. Biol. Chem.* **278**, 19777–19783
8. Costantini, C., Weindruch, R., Della Valle, G., and Puglielli, L. (2005) *Biochem. J.* **391**, 59–67
9. Costantini, C., Scoble, H., and Puglielli, L. (2006) *EMBO J.* **25**, 1997–2006
10. Puglielli, L. (2008) *Neurobiol. Aging* **29**, 795–811
11. Puglielli, L., Konopka, G., Pack-Chung, E., Ingano, L. A., Berezovska, O., Hyman, B. T., Chang, T. Y., Tanzi, R. E., and Kovacs, D. M. (2001) *Nat. Cell Biol.* **3**, 905–912
12. Ko, M. H., and Puglielli, L. (2007) *J. Biol. Chem.* **282**, 19742–19752
13. Zhao, J., Fu, Y., Yasvoina, M., Shao, P., Hitt, B., O'Connor, T., Logan, S., Maus, E., Citron, M., Berry, R., Binder, L., and Vassar, R. (2007) *J. Neurosci.* **27**, 3639–3649
14. Livak, K. J., and Schmittgen, T. D. (2001) *Methods (San Diego)* **25**, 402–408
15. Popsueva, A. E., Luchinskaya, N. N., Ludwig, A. V., Zinovjeva, O. Y., Poteryaev, D. A., Feigelman, M. M., Ponomarev, M. B., Berekelya, L., and Belyavsky, A. V. (2001) *Dev. Biol.* **234**, 483–496
16. Horton, P., Park, K. J., Obayashi, T., Fujita, N., Harada, H., Adams-Collier, C. J., and Nakai, K. (2007) *Nucleic Acids Res.* **35**, W585–W587
17. Nakai, K., and Horton, P. (1999) *Trends Biochem. Sci.* **24**, 34–36
18. Benjannet, S., Elagoz, A., Wickham, L., Mamarbachi, M., Munzer, J. S., Basak, A., Lazure, C., Cromlish, J. A., Sisodia, S., Checler, F., Chretien, M., and Seidah, N. G. (2001) *J. Biol. Chem.* **276**, 10879–10887
19. Hartmann, E., Rapoport, T. A., and Lodish, H. F. (1989) *Proc. Natl. Acad. Sci. U. S. A.* **86**, 5786–5790
20. Carey, D. J., and Hirschberg, C. B. (1981) *J. Biol. Chem.* **256**, 989–993
21. Puglielli, L., Mandon, E. C., and Hirschberg, C. B. (1999) *J. Biol. Chem.* **274**, 12665–12669
22. Puglielli, L., Mandon, E. C., Rancour, D. M., Menon, A. K., and Hirschberg, C. B. (1999) *J. Biol. Chem.* **274**, 4474–4479
23. Maier, B., Gluba, W., Bernier, B., Turner, T., Mohammad, K., Guise, T., Sutherland, A., Thorner, M., and Scoble, H. (2004) *Genes Dev.* **18**, 306–319
24. Han, X., Holtzman, D. M., McKeel, D. W., Jr., Kelley, J., and Morris, J. C. (2002) *J. Neurochem.* **82**, 809–818
25. Cutler, R. G., Kelly, J., Storie, K., Pedersen, W. A., Tammara, A., Hatanpaa, K., Troncoso, J. C., and Mattson, M. P. (2004) *Proc. Natl. Acad. Sci. U. S. A.* **101**, 2070–2075
26. Hodawadekar, S. C., and Marmorstein, R. (2007) *Oncogene* **26**, 5528–5540
27. Thompson, P. R., Wang, D., Wang, L., Fulco, M., Pediconi, N., Zhang, D.,

ATase1 and ATase2 Acetylate Nascent BACE1

- An, W., Ge, Q., Roeder, R. G., Wong, J., Levrero, M., Sartorelli, V., Cotter, R. J., and Cole, P. A. (2004) *Nat. Struct. Mol. Biol.* **11**, 308–315
28. Karanam, B., Jiang, L., Wang, L., Kelleher, N. L., and Cole, P. A. (2006) *J. Biol. Chem.* **281**, 40292–40301
29. Wade, P. A., Pruss, D., and Wolffe, A. P. (1997) *Trends Biochem. Sci.* **22**, 128–132
30. Kouzarides, T. (2000) *EMBO J.* **19**, 1176–1179
31. Sadoul, K., Boyault, C., Pabion, M., and Khochbin, S. (2007) *Biochimie (Paris)* **90**, 306–312
32. Yang, X. J., and Gregoire, S. (2007) *EMBO Rep.* **8**, 556–562
33. Schwer, B., Bunkenborg, J., Verdin, R. O., Andersen, J. S., and Verdin, E. (2006) *Proc. Natl. Acad. Sci. U. S. A.* **103**, 10224–10229
34. Perrimon, N., and Bernfield, M. (2000) *Nature* **404**, 725–728
35. Kenyon, C. (2005) *Cell* **120**, 449–460
36. Longo, V. D., and Finch, C. E. (2003) *Science* **299**, 1342–1346
37. Tissenbaum, H. A., and Guarente, L. (2002) *Dev. Cell* **2**, 9–19